Chem. Senses 36: 389–403, 2011

doi:10.1093/chemse/bjq148
Advance Access publication February 21, 2011

Involvement of NADPH-Dependent and cAMP-PKA Sensitive H^+ Channels in the Chorda Tympani Nerve Responses to Strong Acids

John A. DeSimone, Tam-Hao T. Phan, Gerard L. Heck, ZuoJun Ren, Jamison Coleman, Shobha Mummalaneni, Pamela Melone and Vijay Lyall

Department of Physiology and Biophysics, Virginia Commonwealth University, 1220 East Broad Street, Richmond, VA 23298, USA

Correspondence to be sent to: Dr Vijay Lyall, Department of Physiology and Biophysics, Virginia Commonwealth University, Molecular Medical Research Building (MMRB) #5052, 1220 East Broad Street, Richmond, VA 23219, USA. e-mail: vlyall@vcu.edu

Accepted December 30, 2010

Abstract

To investigate if chorda tympani (CT) taste nerve responses to strong (HCl) and weak (CO_2 and acetic acid) acidic stimuli are dependent upon NADPH oxidase–linked and cAMP-sensitive proton conductances in taste cell membranes, CT responses were monitored in rats, wild-type (WT) mice, and $gp91^{phox}$ knockout (KO) mice in the absence and presence of blockers (Zn^{2+} and diethyl pyrocarbonate [DEPC]) or activators (8-(4-chlorophenylthio)-cAMP; 8-CPT-cAMP) of proton channels and activators of the NADPH oxidase enzyme (phorbol 12-myristate 13-acetate [PMA], H_2O_2, and nitrazepam). Zn^{2+} and DEPC inhibited and 8-CPT-cAMP, PMA, H_2O_2, and nitrazepam enhanced the tonic CT responses to HCl without altering responses to CO_2 and acetic acid. In KO mice, the tonic HCl CT response was reduced by 64% relative to WT mice. The residual CT response was insensitive to H_2O_2 but was blocked by Zn^{2+}. Its magnitude was further enhanced by 8-CPT-cAMP treatment, and the enhancement was blocked by 8-CPT-adenosine-3′-5′-cyclic monophospho-rothioate, a protein kinase A (PKA) inhibitor. Under voltage-clamp conditions, before cAMP treatment, rat tonic HCl CT responses demonstrated voltage-dependence only at ±90 mV, suggesting the presence of H^+ channels with voltage-dependent conductances. After cAMP treatment, the tonic HCl CT response had a quasi-linear dependence on voltage, suggesting that the cAMP-dependent part of the HCl CT response has a quasi-linear voltage dependence between +60 and −60 mV, only becoming sigmoidal when approaching +90 and −90 mV. The results suggest that CT responses to HCl involve 2 proton entry pathways, an NADPH oxidase–dependent proton channel, and a cAMP-PKA sensitive proton channel.

Key words: cAMP, $gp91^{phox}$, PKA, PMA, Rp-cAMPS, sour taste

Introduction

Sour taste is uniquely elicited by acidic stimuli. In the taste bud, the type III cells (or the presynaptic cells) that express the polycystic kidney disease–like proteins, PKD1L3 and PKD2L1, function as sour-sensing cells (Huang et al. 2006, 2008; Ishimaru et al. 2006; LopezJimenez et al. 2006; Roper 2007; Kataoka et al. 2008; Chandrashekar et al. 2009; Ishimaru and Matsunami 2009; Huque et al. 2009). PKD2L1 (Horio et al. 2010) but not the PKD1L3 protein is essential for normal sour taste transduction in the anterior tongue innervated by the chorda tympani (CT) taste nerve (Huang et al. 2006; Yoshida et al. 2009; Horio et al. 2010; Nelson et al. 2010). Both strong and weak organic acids taste sour to humans; however, their transduction mechanisms are quite different. For strong acids that are completely ionized, sour taste transduction depends upon the influx of dissociated H^+ ions through putative apical proton conductive pathways. Most weak organic acids permeate the lipid bilayer of the apical membrane of type III taste cells as undissociated neutral molecules. Once inside the cells they dissociate to generate intracellular H^+ ions. Thus, for both strong acids and weak organic acids, a decrease in the intracellular pH (pH_i) of type III taste cells is the proximate stimulus for sour taste transduction (DeSimone and Lyall 2006; Roper 2007). Following a decrease in taste cell pH_i, the downstream intracellular signaling effectors for sour taste transduction involve cell shrinkage (Lyall et al. 2006), an increase in intracellular Ca^{2+} ($[Ca^{2+}]_i$) (Lyall, Alam, Phan, Phan, et al. 2002; Richter et al. 2003; Huang et al. 2008), and the activation of the basolateral Na^+-H^+ exchanger-1 (NHE-1) which determines the

level of adaptation to the sour stimulus (Lyall, Alam, Phan, Phan, et al. 2002; Lyall, Alam, et al. 2004). However, at present, the putative proton conductive pathways that facilitate the entry of H^+ across the apical membrane of taste cells and their functional role in sour taste transduction have not been elucidated.

NADPH oxidase–linked voltage-gated proton channels are present in phagocytes and nonphagocytic cells and are involved in maintaining pH_i in neutrophils during phagocytosis (Ramsey et al. 2009; Morgan et al. 2009; Musset et al. 2009, 2010; DeCoursey 2010). Proton channels demonstrate perfect selectivity for H^+ with very low single channel currents and are inhibited by Zn^{2+} and diethyl pyrocarbonate (DEPC). The voltage-dependence of the expressed proton channels is strongly modulated by the external pH (pH_o) and pH_i. In this paper, we tested the possibility that an NADPH-linked proton channel is involved in transducing CT responses to strong acids. The CT responses were monitored in Sprague-Dawley rats, wild-type (WT) mice, and NADPH oxidase–knockout (KO) mice containing the null allele of the gene encoding the 91 kD subunit ($gp91^{phox}$) of the oxidase cytochrome *b*. The CT responses were recorded either under open-circuit conditions or under lingual voltage-clamp conditions (Lyall et al. 2006) while the anterior tongue was stimulated with strong acids (HCl or H_3PO_4) or weak organic acids (acetic acid or CO_2). Our results show that approximately 64% of the tonic CT response to HCl depends upon apical H^+ flux through a NADPH oxidase–dependent proton conductance. About 36% of the HCl CT response depends upon an NADPH oxidase–independent proton conductance that is further upregulated by cAMP-protein kinase A (PKA) sensitive mechanism described earlier (Lyall, Alam, Phan, Phan, et al. 2002; Lyall, Alam, et al. 2004; DeSimone et al. 2007). Some of the data in this paper have been published earlier as an abstract (DeSimone et al. 2007).

Materials and methods

CT taste nerve recordings

The animals were housed in the Virginia Commonwealth University animal facility in accordance with institutional guidelines. All in vivo animal protocols were approved by the Institutional Animal Care and Use Committee of Virginia Commonwealth University. Female Sprague-Dawley rats (150–200 g) were anesthetized by intraperitoneal injection of pentobarbital (60 mg/Kg) and supplemental pentobarbital (20 mg/Kg) was administered as necessary to maintain surgical anesthesia. The animal's corneal reflex and toe-pinch reflex were used to monitor the depth of surgical anesthesia. Body temperatures were maintained at 36–37 °C with an isothermal pad (Braintree Scientific). The left CT nerve was exposed laterally as it exited the tympanic bulla and placed onto a 32G platinum/iridium wire electrode. Stimulus solutions maintained at room temperature were injected into a Lucite chamber (3 mL; 1 mL/s) affixed by vacuum to a 28 mm^2 patch of anterior dorsal lingual surface. The CT responses were recorded under zero lingual current-clamp or voltage-clamp conditions and analyzed as described previously (Ye et al. 1991; Lyall, Alam, et al. 2004; Lyall, Heck, et al. 2004; Lyall et al. 2006, 2009). Typically, stimulus solutions remained on the tongue for 1–2 min. Control stimuli consisting of 300 mM NH_4Cl and 300 mM NaCl (Table 1) applied at the beginning and at the end of experiment were used to assess preparation stability (Figures 1C and 4A, Supplementary Figures 2 and 3A). The preparation was considered stable only if the difference between the magnitude of the control stimuli at the beginning and at the end of the experiment was less than 10% (Lyall et al. 2009).

WT female mice (C57BL/6J) and NADPH oxidase KO mice (B6.129S6-$Cybb^{tm1Din}$/J; N13F24) containing the null allele of the gene encoding the 91 kD subunit ($gp91^{phox}$) of the oxidase cytochrome *b* (The Jackson Laboratory) were anesthetized by intraperitoneal injection of pentobarbital (30 mg/Kg) and supplemental pentobarbital (10 mg/Kg) was administered as necessary to maintain surgical anesthesia. The rest of the procedure was the same as in rats except that a flow chamber was not used and stimuli were permitted to flow (3 mL; 1 mL/s) directly across the tongue. At the end of each experiment, animals were killed by an intraperitoneal overdose of pentobarbital (ca. 195 mg/Kg body weight for rats and 150 mg/Kg weight for mice). The composition of the various stimulating solutions used in the CT experiments is given in Table 1. The various drugs and their concentrations used in this study and their specific targets are listed in Table 2.

The sulfhydryl groups on cysteine and the imidazole nitrogen on histidine (His), as well as the carboxylate oxygens of glutamate and aspartate participate in the putative H^+ channel conductance or the H^+-binding site on the channel proteins (Mankelow and Henderson 2001; Seebungkert and Lynch 2001; Lyall, Alam, Phan, Russell, et al. 2002). Voltage-gated proton channels are strongly inhibited by Zn^{2+}, which binds to His residues in the channel protein (Musset et al. 2010). Accordingly, we used the lingual voltage-clamp technique in combination with the pharmacological blockers of proton channels (Zn^{2+} and DEPC) to test if H^+ influx through apical voltage-gated proton channels in taste cells plays a role in eliciting CT responses to strong acids. In some studies, we topically applied 15 mM 8-CPT-cAMP (dissolved in dimethyl sulfoxide [DMSO]) to the lingual surface for 20 min to enhance proton conductance in the apical membrane of taste cells (Lyall, Alam, Phan, Phan, et al. 2002; Lyall, Alam, et al. 2004). To test if cAMP modulates proton conductances directly or produces its effect indirectly by activating PKA, Rp-cAMPS, a specific membrane permeable inhibitor of PKA I and II activation by cAMP (Botelho et al. 1988) was applied topically (4.5 mM;

Table 1 Composition of stimulating solutions for CT experiments

Solution	Composition (mM)	pH
Rinse (R1)	10 KCl	
Acid stimuli	20 HCl, 20 H_3PO_4, 20 CH_3COOH	1.7, 2.3, 3.2
Rinse (R2)	72 KCl + 10 HEPES	7.4
10% CO_2	72 $KHCO_3$ + 10% CO_2/90% O_2	7.4
Rinse (R3)	525 CH_3COOK + 30 mannitol + 10 HEPES	6.1
CH_3COOH	525 CH_3COOK + 30 CH_3COOH	6.1
Control-1	300 NH_4Cl	
Control-2	300 NaCl	
Ringer's solution	140 NaCl + 5 KCl + 1 $CaCl_2$ + 1 $MgCl_2$ + 10 Na-pyruvate + 10 glucose + 10 HEPES	7.4

HEPES, *N*-2-hydroxyethylpiperazine-*N*′-2-ethanesulfonic acid. Mannitol was added to maintain R3 and CH_3COOH stimulus solutions at the same osmotic pressure. Mannitol by itself does not elicit a CT response (Lyall et al. 2006).

dissolved in DMSO) to the tongue for 10 min. As a control, we used 15 mM 8-CPT-cGMP (Table 2). NADPH oxidase–linked proton channels in phagocytes and other tissues are modulated by free radicals, nitrazepam, and phorbol 12-myristate 13-acetate (PMA; DeCoursey 2003). To test if acid responses depend upon H^+ influx through NADPH oxidase–linked proton channels, nitrazepam (a synthetic substrate for intracellular NADPH oxidase (Rosen et al. 1984) and PMA (dissolved in DMSO) were applied topically to the tongue for 15 min. H_2O_2 was added directly to the rinse solution and the sour stimuli (Table 2). NADPH oxidase KO mice were used to test if acid responses depend upon H^+ influx through NADPH oxidase–linked proton channels.

Data analysis

In CT experiments, the tonic (steady state) part of acid-evoked neural responses was quantified by taking the area under the response curve over the final 30 s of a stimulation. To normalize this result, this area was divided by the area

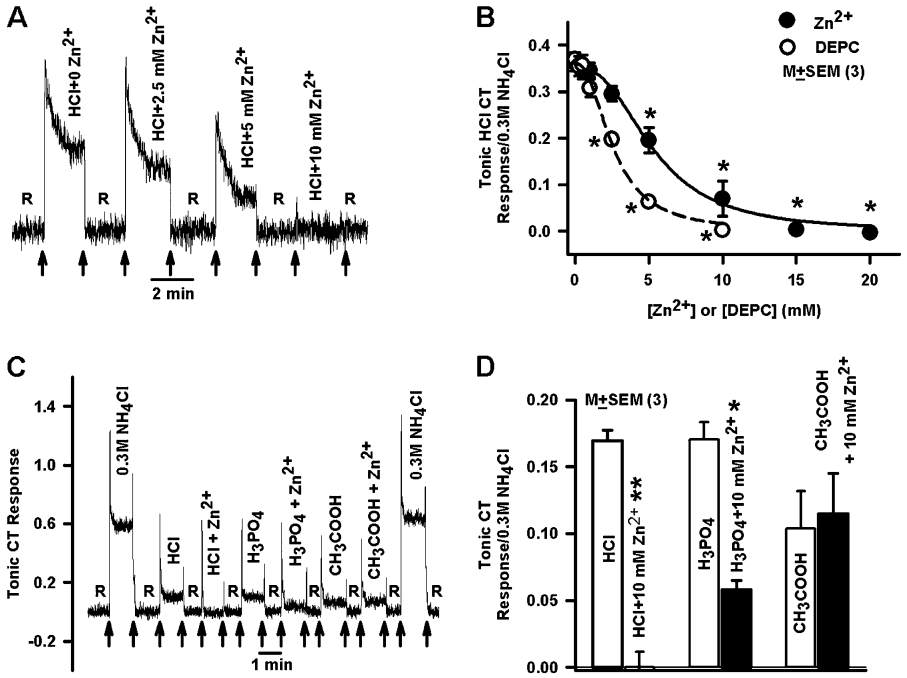

Figure 1 Effects of Zn^{2+} and DEPC on rat CT responses to acidic stimuli. **(A)** Shows a representative CT recording in which the rat tongue was first superfused with a rinse solution R1 (10 mM KCl) and then with 20 mM HCl solutions containing 0, 2.5, 5.0, and 10.0 mM $ZnCl_2$. The arrows indicate the time period when the tongue was stimulated with different solutions. **(B)** The mean normalized tonic CT response in 3 rats to 20 mM HCl were plotted as a function of either Zn^{2+} (●) or DEPC (○) concentration. The tonic HCl CT responses at 10, 15, and 20 mM Zn^{2+} and 10 mM DEPC were not different from the baseline rinse values ($P > 0.05$). The P values were calculated with respect to the normalized HCl tonic CT response in the absence of Zn^{2+} or DEPC. The P values (*) at different Zn^{2+} concentration were 5 mM (0.0075), 10 mM (0.0023), 15 mM (0.0001), and 20 mM (0.0001) relative to control (0 Zn^{2+}). The P values (*) at different DEPC concentration were 2.5 mM (0.0007), 5 mM (0.0001), and 10 mM (0.0001). **(C)** Shows a representative CT recording in which the rat tongue was first superfused with a rinse solution R1 (10 mM KCl) and then with acidic stimuli (20 mM HCl, 20 mM H_3PO_4, and 20 mM CH_3COOH) in the absence and presence of 10 mM $ZnCl_2$ (Zn^{2+}). The control responses to 300 mM NH_4Cl are shown at the beginning and end of the experiment and were nearly identical. The arrows indicate the time period when the tongue was stimulated with different solutions. **(D)** The mean normalized tonic CT response in 3 rats to 20 mM HCl, 20 mM H_3PO_4, and 20 mM CH_3COOH are shown in the absence and presence of 10 mM $ZnCl_2$ (Zn^{2+}). The tonic CT response to HCl + Zn^{2+} was inhibited to the baseline rinse values (**$P = 0.0004$). There was no difference between the tonic CT response between CH_3COOH and CH_3COOH + Zn^{2+} ($P > 0.05$). Zn^{2+} inhibited the tonic CT response to H_3PO_4 by 65.8% (*$P = 0.0016$).

Table 2 Summary of the effect of various drugs used in this study that modulate gp91^{phox}- and cAMP PKA–dependent proton channels

Drug	mM	Intracellular targets
Zn^{2+}	0–20	↓Proton channels
DEPC	0–10	↓Proton channels
8-CPT-cAMP	15	↑Proton channel activity
8-CPT-cGMP	15	
H_2O_2	0–15%	↑Proton channel activity
Nitrazepam	0.5	Synthetic substrate for intracellular NADPH oxidase
PMA	0.25	↑Proton channels in phagocytes
Rp-8-CPT-cAMPS	4.5	↓PKA I and II

PMA (activates protein kinase C); 8-CPT-cAMP, 8-(4-chlorophenylthio) adenosine-3′-5′-cyclic monophosphate (membrane permeable cAMP analog); Rp-8-CPT-cAMPS, 8-(4-chlorophenylthio)-adenosine-3′-5′-cyclic monophospho-rothioate (competitive inhibitor of PKA I and II); 8-CPT-cGMP, 8-(4-chlorophenylthio) guanosine-3′-5′-cyclic monophosphate (membrane permeable cGMP analog); and DEPC (modification reagent for His and Tyr residues in proteins). All reagents were obtained from Sigma.

under the 300 mM NH_4Cl response curve over the final 30 s of the response period. The normalized data were reported as the mean ± standard error of the mean of the number of animals. To facilitate comparison of the CT responses in WT and NADPH oxidase KO mice, the data traces in each experiment were digitally normalized by dividing the digitized responses to each test stimulus in a given mouse by the mean tonic response of the mouse to 300 mM NH_4Cl. Because we are comparing the normalized CT responses before and after the topical lingual application of pharmacological modulators in the same CT preparation, a paired *t*-test was used to evaluate statistical significance. When the data were compared between different genotypes, an unpaired *t*-test was used.

Detection of gp91^{phox} in WT mouse fungiform taste bud cells and control kidney cells

The reverse transcription (RT)-polymerase chain reaction (PCR) technique was utilized to detect the presence of gp91^{phox} in fungiform (FF) taste bud cells. WT mice were anesthetized by exposing them to an inhalation anesthetic, isoflurane (1.5 mL) in a desiccator. When the mice were fully unconscious, a midline incision was made in the chest wall and the aorta severed. The tongue and kidneys were then rapidly removed and stored in ice-cold Ringer's solution (Table 1). The lingual epithelium was isolated by collagenase treatment as described earlier (Lyall, Heck, et al. 2004). Taste buds were harvested from FF papillae, aspirated with a micropipette. The taste buds were first individually transferred onto coverslips, avoiding contaminating cells and debris and then transferred into tubes for RNA preparation. RNA was prepared using the RNeasy Protect Kit (Qiagen) and the cDNA was generated using the M-MLV Reverse Transcriptase Kit (Invitrogen) according to the manufacturer's protocols. PCR screening of the FF and kidney cDNAs for the presence of mouse gp91^{phox} was performed with *Taq* DNA Poymerase (Roche) using the primer pairs (Invitrogen) shown below. The reaction was performed at the annealing temperatures of 53, 54 and 55 °C. As a negative control, the reactions were run with water replacing the cDNA template. Primer sequences for mouse gp91^{phox} (NM_007807) were as described elsewhere (Wu et al. 2006). The forward primer site spans the exon that ends at 1226 bp and the reverse spans the exon that ends at 1536. The primers were designed to cover exon splice sites so that genomic contamination is not an issue.

Primer pair

Sense: 5′-CAGGAGTTCCAAGATGCCTG-3′
Antisense: 5′-GATTGGCCTGAGATTCATCC-3′
Product size: 349 bp

Results

Effect of Zn^{2+} and DEPC on CT responses to acidic stimuli

Adding increasing concentrations of $ZnCl_2$ (2.5–10 mM) to 20 mM HCl solution inhibited the HCl CT response in a dose-dependent manner (Figure 1A). The concentration–response curve for Zn^{2+} inhibition of the HCl CT response is shown in Figure 1B. The solid curve is the least squares fit of the data according to a reversible competitive inhibition model (Appendix eq. 5, with $R_m = 0.351$, $k = 5.3$ mM, and $n = 2.6$). At concentrations ≥10 mM, Zn^{2+} inhibited the mean normalized tonic CT response to HCl to rinse baseline level (Figure 1B; ●). When added to the rinse solution (R1; Table 1), Zn^{2+} (2.5–20 mM) did not give a CT response above the rinse baseline level (data not shown).

Although Zn^{2+} (10 mM) inhibited the tonic CT response to 20 mM HCl to rinse baseline level, it had no effect on the tonic CT response to 20 mM acetic acid and only partially inhibited the CT response to 20 mM H_3PO_4 (Figure 1C). The effect of Zn^{2+}on these 3 acids is quantified in Figure 1D. Zn^{2+} at 10 mM completely inhibited the mean normalized tonic HCl CT response. It inhibited the mean normalized tonic CT response to H_3PO_4 by 65.6% relative to control, and it had no effect on the CT response to acetic acid (Figure 1D) or 10% CO_2 (pH 7.4) (data not shown). Thus, unlike HCl, CT responses to H_3PO_4 depend both upon H^+ entry through the Zn^{2+}-sensitive proton channels and on the passive diffusion of H_3PO_4 as the undissociated acid. The proportion of the H_3PO_4 CT response inhibited by Zn^{2+} is very close to the calculated percentage of the dissociated form of the acid present in the solution. For 20 mM H_3PO_4 at the measured pH of 2.3, the percent of the acid in the dissociated form ($H_2PO_4^-$) is about 60%.

DEPC inhibited the HCl CT response in a dose-dependent manner (Supplementary Figure 1A). Figure 1B shows that inhibition by DEPC can also be modeled as reversible

competitive inhibition (Appendix eq. 5 with $R_m = 0.361$, $k = 2.6$ mM, and $n = 2.3$). A comparison of the dissociation constants for Zn^{2+} and DEPC inhibition shows that DEPC is a somewhat more effective antagonist inhibiting 50% of the response to HCl at half the concentration required when using Zn^{2+}. DEPC (10 mM) inhibited the tonic HCl CT response to baseline. Although not shown in the figure, DEPC inhibition was completely reversible. By itself, DEPC (1–10 mM) added to the rinse solution elicited no CT response above the rinse baseline level (Lyall, Alam, Phan, Russell, et al. 2002). DEPC had no effect on the CT response to 10% CO_2 (pH 7.4; Table 1) (Supplementary Figure 1B). The mean normalized tonic CT response to CO_2 was the same in the absence and the presence of DEPC in the stimulus solution (Supplementary Figure 1C). Thus, blocking the apical membrane proton conductance in taste cells with Zn^{2+} or DEPC produces similar effects on the HCl CT responses.

Effect of voltage clamping the chemically stimulated receptive field on the HCl CT response

Consistent with earlier studies (DeSimone et al. 1995), voltage clamping the chemically stimulated receptive field between +60 and –60 mV did not produce a significant change in the tonic HCl CT response relative to its value under open-circuit conditions (Figure 2A; ○). However, the HCl tonic CT response was significantly enhanced at –90 mV and significantly suppressed at +90 mV relative to its value under open-circuit conditions (Figure 2A; ○). This nonlinear CT response versus voltage curve can be represented using a standard ion channel kinetic model but not without assuming a voltage-dependent rate constant for the dissociation of the proton-channel complex (cf. Appendix). Accordingly, the Appendix equations (2) and (3) were used to compute the least squares curve fitted to the open circles in Figure 2A ($\beta = 0.39$, $a = 100$, $\delta = 0.91$, $\tau = -3.9$, $n = 3$). In the presence of 20 mM Zn^{2+}, the mean normalized CT response to HCl was inhibited to baseline under open-circuit conditions (Figure 2B; Control; 0 mV), and in the continuous presence of Zn^{2+}, no voltage-induced effects could be observed on the tonic CT response at +90 or –90 mV applied lingual potential (Figure 2B; Control). These results are consistent with the presence of a Zn^{2+}-sensitive apical proton conductance in taste cells. In contrast to Zn^{2+}, an equivalent concentration of $CaCl_2$ or $MgCl_2$ produced no effect on the mean normalized tonic HCl CT response (Figure 2C). This suggests that inhibition of the HCl CT response by Zn^{2+} is not explained solely by its divalent properties.

Effect of cAMP on the HCl CT response

Topical lingual application of 8-CPT-cAMP enhanced the CT response to 20 mM HCl (0 mV; Figure 2A; Post-cAMP; ●) relative to control (0 mV; Figure 2A; Control; ○). The post-cAMP HCl CT response demonstrated a quasi-linear voltage dependence over voltages from +90 to –90 mV (Figure 2A; Post-cAMP; ●). The difference in the CT response in the presence and absence of cAMP at each voltage represents the cAMP-dependent part of the response and is plotted in Figure 2A as closed triangles. The cAMP-dependent part of the response was fitted according to the standard ion channel kinetic model without further assumptions, that is, the respective rate constants for the formation of the channel-H^+ complex and its dissociation are voltage independent (Appendix eq. 2, $R_m = 0.52$, $a = 2.6$, $\delta = 0.69$). The cAMP-dependent part of the response is seen to be quasi-linear between ±60 mV becoming slightly sigmoidal between 60 and 90 mV and –60 and –90 mV. For this reason, the curve fitting the post-cAMP CT response (which is the sum of the cAMP-dependent and -independent curves) is seen to be essentially quasi-linear. Both the cAMP-induced increase in the HCl CT response and the observed enhanced voltage sensitivity were inhibited to the rinse baseline level in the presence of 20 mM Zn^{2+} (Figure 2B; Post-cAMP, hatched bars). In contrast to cAMP, topical lingual application of an equivalent concentration of 8-CPT-cGMP failed to produce any effects on the CT responses to 100 mM NaCl, 100 mM NH_4Cl, 100 mM KCl, or 20 mM HCl (Supplementary Figure 2A,B). These results indicate that a Zn^{2+}-sensitive apical H^+ conductive pathway in taste cells is specifically modulated by cAMP.

Effect of the modulators of proton channels in phagocytes on the HCl CT response

Stimulating the tongue with 20 mM HCl containing H_2O_2 (5–15%) increased the magnitude of the CT response to HCl in a concentration-dependent manner (Supplementary Figure 3). When added to the rinse solution, H_2O_2 by itself gave a small but significant CT response. The mean normalized HCl CT responses in the presence of H_2O_2 were calculated with respect to the baseline obtained after superfusing the tongue with rinse solution (R1) containing the same concentration of H_2O_2. H_2O_2 enhanced the mean normalized HCl CT response in a concentration-dependent manner, saturating at H_2O_2 concentrations above 8% (Figure 3A). The saturating sigmoidal curve through the points in Figure 3A is the least squares fit of the data to the Hill equation (Appendix eq. 6, $R_0 = 0.147$, $R_1 = 0.135$, $k_{0.5} = 4.6$, and $n = 5.6$). The mean normalized tonic CT responses to 30 mM acetic acid buffered to pH 6.1 with CH_3COOK or 10% CO_2 buffered to pH 7.4 with $KHCO_3$ (Table 1) were unaffected by H_2O_2 (Figure 3B). These results indicate that H_2O_2 specifically enhances the CT response to HCl.

Topical lingual application of 0.5 mM nitrazepam enhanced the CT response to HCl but not the CT response to CO_2 or acetic acid (Figure 4A). The mean normalized tonic CT response to CO_2 or acetic acid was unaffected by nitrazepam (Figure 4B; Post-nitrazepam). In another set of rats, topical lingual application of 0.25 mM PMA significantly enhanced the magnitude of the CT response to 20 mM HCl relative to control (Figure 4C). Consistent with previous studies with PMA in taste cells (Lyall et al. 2009), the

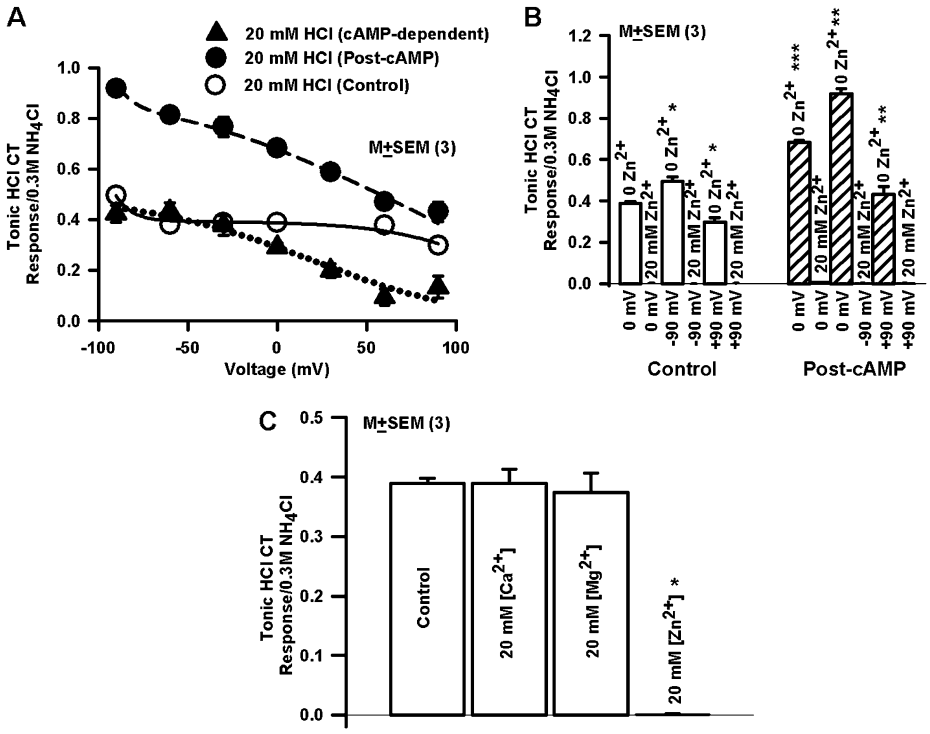

Figure 2 Effects of lingual voltage clamp, cAMP, and Zn^{2+} on the rat HCl CT response. **(A)** Rat CT responses 20 mM HCl were monitored at applied +90, +60, +30, 0, −30, −60, and −90 mV across the receptive field under control conditions and after topical lingual application of 15 mM 8-CPT-cAMP for 20 min. The mean normalized tonic HCl CT responses in 3 rats are plotted as a function of the applied voltage before (o; Control) and after cAMP treatment (●; Post-cAMP). The cAMP-dependent mean tonic responses (▲; cAMP dependent) at each applied voltage were calculated as the difference between the HCl CT response before and after cAMP treatment. The data points were fitted to the channel model described in the Appendix. **(B)** The mean normalized tonic CT responses in rats to 20 mM HCl and 20 mM HCl + 20 mM $ZnCl_2$ are shown at +90, 0, and −90 mV applied voltage across the receptive field. cAMP significantly enhanced the HCl CT response at +90, 0, and −90 mV relative to control. Under control conditions, the *P* values were calculated with reference to the mean normalized tonic HCl CT response at 0 mV. The *P* values (*) at −90 and +90 mV were 0.0102 and 0.0158, respectively. Cyclic-AMP enhanced the HCl CT response at 0 mV relative to control (***$P = 0.0001$). Post-cAMP, the *P* values (**) at −90 and +90 mV were 0.001 and 0.0034, respectively with respect of 0 mV. Zn^{2+} inhibited the HCl CT responses at +90, 0, and −90 mV to the rinse baseline under control conditions and after cAMP treatment, ($P > 0.05$ with respect to zero). **(C)** Effect of Ca^{2+}, Mg^{2+}, and Zn^{2+} on the rat HCl CT response. The rat tongues were first superfused with a rinse solution R1 (10 mM KCl) and then with 20 mM HCl solutions containing 20 mM $CaCl_2$, 20 mM $MgCl_2$, or 20 mM $ZnCl_2$. Addition of 20 mM $CaCl_2$, 20 mM $MgCl_2$, or 20 mM $ZnCl_2$ to R1 did not increase the CT response above baseline relative to R1 alone (data not shown). The mean normalized tonic HCl CT responses in 3 rats are shown in the presence of Ca^{2+}, Mg^{2+}, and Zn^{2+}. Whereas Zn^{2+} inhibited the mean normalized HCl tonic CT response to baseline (*$P = 0.0001$), Ca^{2+} and Mg^{2+} did not have any effect on the tonic HCl CT response ($P > 0.05$).

effects of PMA were not observed in the presence of the protein kinase C blocker, R031-8220 (data not shown). These data suggest that agents that activate an H^+ channel linked to NADPH oxidase activity in phagocytes also modulate a similar conductance in taste cells.

Detection of gp91^{phox} in FF taste bud cells and kidney cells by RT-PCR

In cDNA made from FF taste bud cells and kidney cells, using specific primer pairs, we detected the message for gp91^{phox}, membrane associated component of NAHPH oxidase in kidney cells, and FF taste bud cells (Supplementary Figure 4). The PCR product (349 bp) was sequenced and was found to match 100% the sequence of gp91^{phox} in the gene bank (NM_007807) (data not shown). These results suggest that gp91^{phox} is most likely expressed in taste cells. To further investigate if the observed apical proton conductance in taste cells is linked to the NADPH oxidase activity, we performed additional studies in NADPH oxidase KO mice.

Responses of WT and NADPH oxidase KO mice to HCl and CO_2

In the gp91^{phox} KO mice (Figure 5B), the normalized HCl tonic CT response was smaller relative to its magnitude in the WT mice (Figure 5A). Zn^{2+} (10 mM) inhibited the HCl CT response in WT mice (Figure 5A) and the residual response (the gp91^{phox}-independent HCl CT response) in KO mice (Figure 5B). Although in WT mice (Figure 5A), the CT response was further enhanced when HCl was presented with 15% H_2O_2, the residual HCl CT response in gp91^{phox} KO mice (Figure 5B) was not affected by stimulating the tongue with 20 mM HCl + 15% H_2O_2. The mean normalized CT responses from several WT and KO mice are summarized in Figure 8.

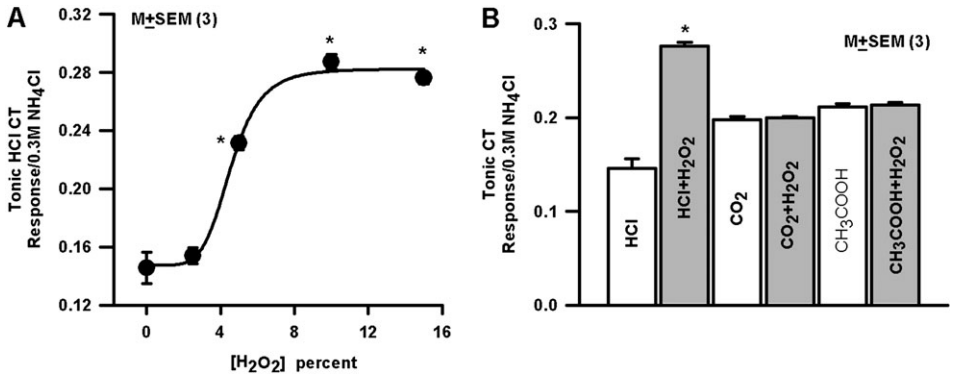

Figure 3 Effect of H_2O_2 on the rat HCl CT response. **(A)** The rat tongues were initially superfused with rinse solutions (R1; Table 1) containing H_2O_2 (R1 + 0, 2.5, 5.0, 10.0, and 15.0% H_2O_2) and then with 20 mM HCl solutions containing H_2O_2 (HCl + 0, 2.5, 5.0, 10.0, and 15.0% H_2O_2), respectively (see also Supplementary Figure 3). The H_2O_2-induced enhancement in the tonic HCl response at a particular H_2O_2 concentration was calculated relative to the baseline with the same H_2O_2 in R1. The mean normalized tonic HCl CT responses in 3 rats are plotted as a function of increasing H_2O_2 concentration. The *P* values were calculated with respect to the mean normalized HCl tonic CT response in the absence of H_2O_2. The *P* values (*) at different H_2O_2 concentrations were as follows: 5% (0.0019), 10% (0.0003), and 15% (0.0003). **(B)** CT responses were monitored while the rat tongues were superfusing with R1 and then with 20 mM HCl, R1 + 15% H_2O_2, and 20 mM HCl + 15% H_2O_2, R2 (pH 7.4) and 10% CO_2 (pH 7.4; Table 1) and R3 (pH 6.1) and 525 mM CH_3COOK + 30 mM CH_3COOH (pH 6.1; Table 1). The mean normalized tonic CT responses in 3 rats to HCl, CO_2, and CH_3COOH are shown in the absence and presence of 15% H_2O_2. H_2O_2 only enhanced CT responses to HCl (*P = 0.0003). No significant difference was observed in the normalized tonic CT response to CO_2 or CH_3COOH ($P > 0.05$).

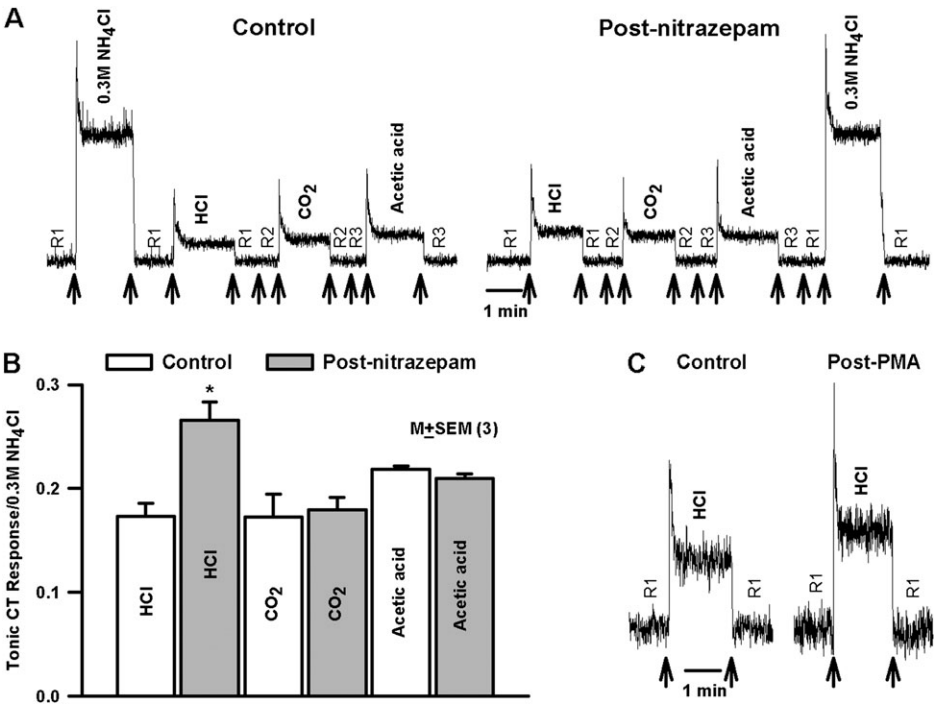

Figure 4 Effect of nitrazepam and PMA on the rat CT responses to acidic stimuli. **(A)** Shows a representative raw neural recording in which CT responses were monitored while the rat tongue was superfusing with R1 and then with 20 mM HCl, R2 and 10% CO_2 (pH 7.4; Table 1), and R3 and 20 mM CH_3COOH (pH 6.1; Table 1) before (Control) and after topical lingual application of 0.5 mM nitrazepam (Post-nitrazepam). The control responses to 300 mM NH_4Cl are shown at the beginning and end of the experiment and were nearly identical. The arrows indicate the time period when the tongue was stimulated with different solutions. **(B)** The mean normalized tonic CT responses in 3 rats to HCl, CO_2, and CH_3COOH are shown before (Control) and after nitrazepam treatment (Post-nitrazepam). Nitrazepam only enhanced HCl CT responses (*P = 0.013). No effect of nitrazepam was observed on the CT responses to CO_2 or CH_3COOH relative to control (P >0.05). (**C**) Shows a representative CT recording in which the rat tongue was first superfused with a rinse solution R1 (10 mM KCl) and then with 20 mM HCl solution under control conditions and after topical lingual application of 0.25 mM PMA. The arrows indicate the time period when the tongue was stimulated with different solutions.

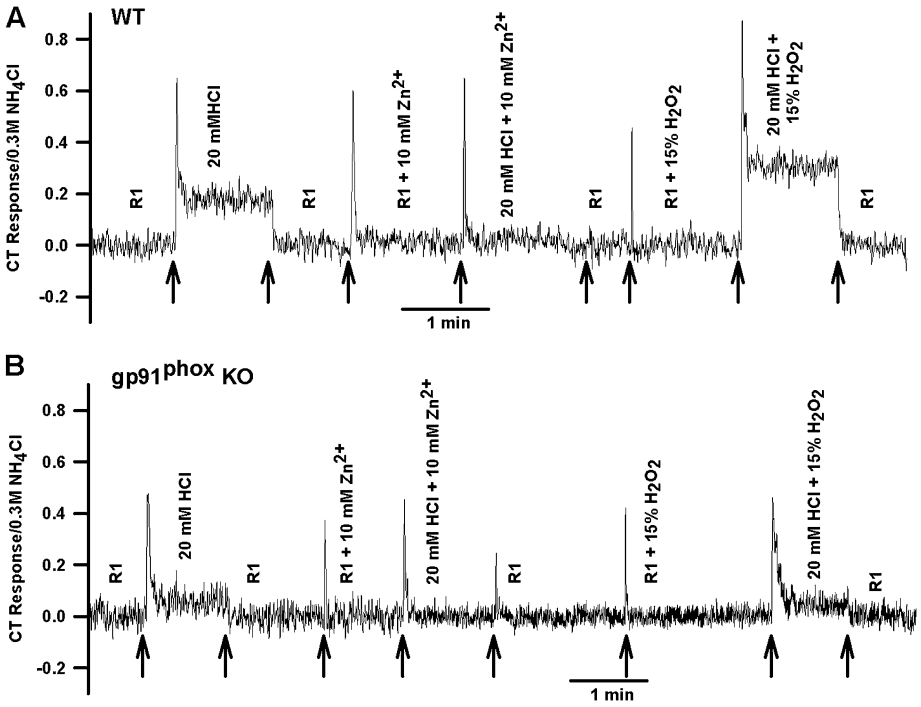

Figure 5 Effect of H_2O_2 and Zn^{2+} on HCl CT responses in WT and gp91^{phox} KO mice. Shows representative normalized CT responses **(A)** in a WT mouse and **(B)** a KO mouse in which the tongues were initially superfused with rinse solutions R1, R1 + 15% H_2O_2, or R1 + 10 mM Zn^{2+} and then with 20 mM HCl, HCl + 15% H_2O_2, or HCl + 10 mM Zn^{2+}. The arrows indicate the time period when the tongues were stimulated with different solutions.

In WT mice (Figures 6A and 8), the tonic CT response to 20 mM HCl was typically greater than the response to 10% CO_2 (pH 7.4). In gp91^{phox} KO mice (Figures 6B and 8), the mean normalized HCl tonic CT response was diminished by about 64% relative to the WT mice and was significantly smaller relative to the response to CO_2 (Figures 6B and 8). Although in the presence of 15% H_2O_2, the CT response to HCl in WT mice was enhanced relative to control, no effect of H_2O_2 was observed on the CT response to 10% CO_2 (Figure 8). As shown before (Figure 5B), the residual HCl CT response in KO mice was insensitive to H_2O_2. Thus, in mice as well as in rats, H_2O_2 only enhanced the CT response to HCl and the response to a weak organic acid (CO_2) is H_2O_2 insensitive.

In contrast to rats (data not shown), some WT and gp91^{phox} KO mice elicited a tonic CT response to 10 mM Zn^{2+} (Figures 5A, 6B, and 7A) to which level the response to HCl was inhibited by Zn^{2+}.

Effect of cAMP on the residual HCl CT response in gp91^{phox} KO mice

H_2O_2 did not affect the residual response to HCl in the gp91^{phox} KO mouse (Figure 7A). Treating the mouse tongue with 8-CPT-cAMP enhanced the residual tonic HCl CT response (Figure 7A). This indicates that cAMP-modulation resides in the H^+ conductance that is distinct from the gp91^{phox} component of NADPH oxidase. We have previously shown that cAMP does not affect CT responses to CO_2 or acetic acid (Lyall, Alam, et al. 2004). Thus data obtained from both rat and KO mouse models demonstrate the presence of 2 distinct H^+ entry pathways in the apical membranes of taste cells that have a direct functional role in the CT response to strong acids.

Effect of Rp-cAMPS on the cAMP-sensitive HCl CT response in rats

The effect of cAMP on the HCl CT response was monitored before and after topical lingual application of Rp-cAMPS. As shown earlier (Figure 2A,B), 8-CPT-cAMP enhanced the rat HCl CT response (Figure 7B). Exposure of the tongue to 8-CPT-cAMP in the Rp-cAMPS pretreated tongues did not produce the expected increase in CT response to HCl (Figure 7C). In 3 rats, the magnitude of the mean normalized tonic CT responses post-Rp-cAMPS and post-Rp-cAMPS-post-CPT-cAMP were not different from their values under control condition ($P > 0.05$; data not shown). These results suggest that cAMP exerts its effect on an apical proton channel through PKA.

Discussion

In rodents, stimulating the tongue with HCl (1–30 mM) elicits concentration-dependent CT responses (Stewart et al. 1998; Lyall, Alam, Phan, Phan, et al. 2002) and induces

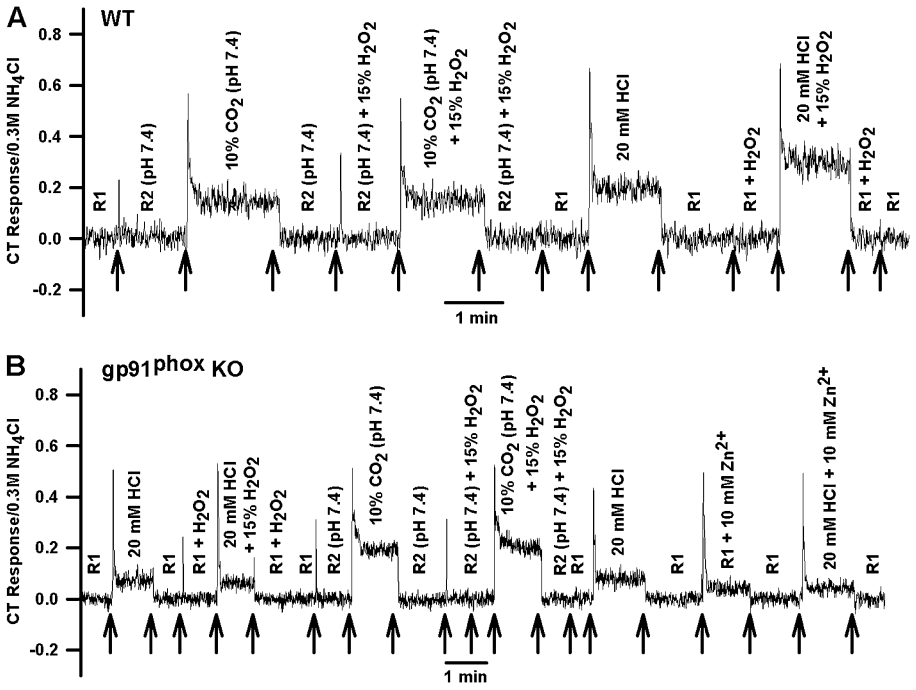

Figure 6 Effect of H_2O_2 on the CT responses to HCl and CO_2 in WT and gp91^{phox} KO mice. Shows representative normalized CT responses **(A)** in a WT mouse and **(B)** a KO mouse in which the tongues were initially superfused with rinse solutions R1, R1 + 15% H_2O_2, R2 (pH 7.4), or R2 + 15% H_2O_2 (pH 7.4; Table 1) and then with 20 mM HCl, HCl + 15% H_2O_2, 10% CO_2 (pH 7.4; Table 1), or 10% CO_2 + 15% H_2O_2 (pH 7.4; Table 1). In **(B)** is also shown the response to R1, R1 + 10 mM Zn^{2+}, 20 mM HCl, and 20 mM HCl + 10 mM Zn^{2+}. The arrows indicate the time period when the tongues were stimulated with different solutions.

a dose-dependent decrease in pH_i in polarized FF taste bud cells in vitro (Lyall, Alam, Phan, Phan, et al. 2002). Our results suggest that at least 2 distinct proton conductive pathways in the apical membrane of taste cells contribute to the HCl CT response. One proton conductive pathway is dependent upon NADPH oxidase activity and is sensitive to Zn^{2+}, DEPC, H_2O_2, PMA, and nitrazepam. H^+ influx into taste cells through this pathway accounts for 64% of the HCl CT response. The second proton conductive pathway is independent of NADPH oxidase activity. It is sensitive to Zn^{2+}, cAMP, and PKA but is insensitive to H_2O_2. Under control conditions, H^+ influx through this pathway accounts for 36% of the HCl CT response. Cyclic AMP enhances H^+ influx through this pathway and increases the HCl CT response. We hypothesize that both NADPH oxidase–dependent and cAMP-sensitive proton channels are present in the PKD2L1 containing sour sensing taste cells in the anterior tongue (Huang et al. 2006; Yoshida et al. 2009; Horio et al. 2010; Nelson et al. 2010; Chang et al. 2010).

NADPH-dependent proton conductance in taste cells

Because stimulating the tongue with HCl elicits a CT response, it suggests that the putative proton channels in the apical membrane of taste cells are constitutively active. Under control conditions (Figure 2A), voltage dependence of the HCl CT response was only observed at +90 and –90 mV (Lyall, Alam, Phan, Phan, et al. 2002; Lyall, Alam, et al. 2004). These results are consistent with the observations that the voltage dependence of voltage-gated proton channels is not absolute (Musset et al. 2009). In our studies, Zn^{2+} blocked both the NADPH oxidase–dependent and NADPH oxidase–independent cAMP-sensitive proton conductances in taste cells (Figures 1, 2, 5, and 6). Proton channels are inhibited by divalent cations. In fact, sensitivity to Zn^{2+} and Cd^{2+} has classically been considered a prerequisite in identifying these channels (Decoursey 2003).

HCl CT responses in rats and WT mice were enhanced in the presence of H_2O_2 (Figures 3 and 5–7), nitrazepam (Figures 4A,B), and PMA (Figure 4C), known activators of the NADPH oxidase in phagocytes and nonphagocyte cells. Most importantly, the HCl CT response was decreased by 64% in gp91^{phox} KO mice (Figure 8). In KO mice, the residual HCl CT response was not affected by H_2O_2 (Figures 5B, 6B, 7A, and 8). These results suggest that in taste cells of KO mice, the NADPH oxidase is completely inhibited. The gp91^{phox} KO mice have been shown to lack NADPH oxidase activity in neutrophils (Malech 1999), astrocytes (Abramov et al. 2005), intrapulmonary arteries (Liu et al. 2006), and the striatum (Clement et al. 2010). Taken together, the above results suggest that a significant part of the apical proton conductance in taste cells is dependent upon the NADPH oxidase activity. A similar cooperative relationship between the voltage-gated proton channels and NADPH oxidase

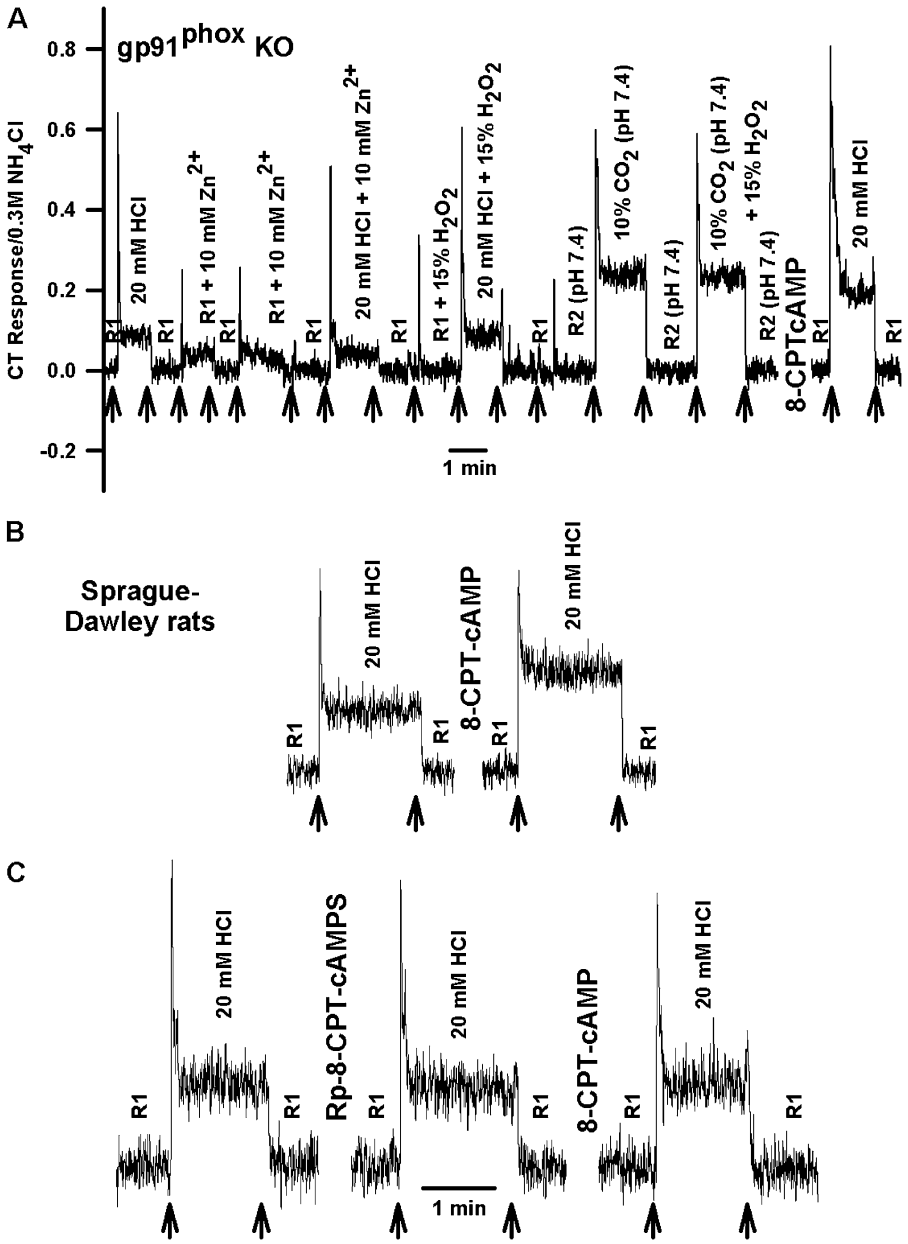

Figure 7 Effect of Zn^{2+}, H_2O_2, and cAMP on the CT responses to HCl and CO_2 in gp91^{phox} KO mice and Sprague-Dawley rats. **(A)** Shows a representative CT recording in a gp91^{phox} KO mouse in which the mouse tongue was initially superfused with R1, R1 + 10 mM Zn^{2+}, R1 + 15% H_2O_2, R2 (pH 7.4), or R2 + 15% H_2O_2 (pH 7.4; Table 1) and then with 20 mM HCl, 20 mM HCl + 10 mM Zn^{2+}, 20 mM HCl+15% H_2O_2, 10% CO_2 (pH 7.4; Table 1) or 10% CO_2 + 15% H_2O_2 (pH 7.4; Table 1). Also shown is the CT response to 20 mM HCl after the topical lingual application of 8-CPT-cAMP. The arrows indicate the time period when the tongue was stimulated with different solutions. **(B)** Shows a representative rat CT recording in which the tongue was first superfused with R1 and then with 20 mM HCl under control conditions and after topical lingual application of 15 mM 8-CPT-cAMP for 20 min. The arrows indicate the time period when the tongues were stimulated with different solutions. **(C)** Shows a representative rat CT recording in which the tongue was first superfused with R1 and then with 20 mM HCl under control conditions, after topical lingual application of 4.5 mM Rp-8-CPT-cAMPS for 10 min and after topical lingual application of 15 mM 8-CPT-cAMP (Table 2). The arrows indicate the time period when the tongues were stimulated with different solutions.

activity has been demonstrated in phagocytes during a respiratory burst when reactive oxygen species are produced to kill microbial invaders (Musset et al. 2009). However, at present it is not clear how NADPH activity is linked to the activation of voltage-gated proton channels. Several speculative explanations for the paradoxical interactions between proton channels and NADPH oxidase have been presented (Musset et al. 2009).

Active NADPH oxidase transfers electrons from the substrate to O_2 forming O_2^-. A defect in any of the genes encoding the components of the NADPH oxidase (viz. gp91^{phox}, p22^{phox}, p67^{phox}, or p47^{phox}) results in a decrease in NADPH

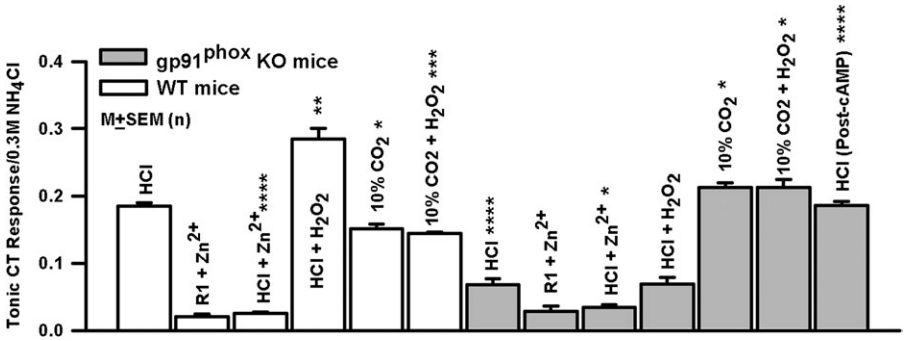

Figure 8 Effects of Zn^{2+}, H_2O_2, and cAMP on the CT responses to acidic stimuli in WT and gp91^{phox} KO mice. In 3 WT mice, the *P* values under different conditions were calculated with respect to the mean normalized tonic HCl CT response and were as follows: HCl + Zn^{2+} (****; 0.0001), HCl + H_2O_2 (**; 0.004), 10% CO_2 (*; 0.0168), and 10% CO_2 + H_2O_2 (***; 0.0014). In 6 KO mice, the *P* values under different conditions were calculated with respect to the mean normalized tonic HCl CT response and were as follows: HCl + Zn^{2+} (*; 0.0276), HCl + H_2O_2 (>0.05), 10% CO_2 (*; 0.0295), 10% CO_2 + H_2O_2 (*; 0.0295) and post-cAMP HCl (****; 0.0001). The mean tonic HCl CT response in KO mice was smaller relative to its value in WT mice (****P = 0.0001).

oxidase activity and a decrease in reactive oxygen species. Homologues of gp91^{phox}, called Nox and Duox, are present in a large variety of nonphagocytic cells. The gp91^{phox} subunit is the electron transport chain of the active NADPH oxidase (Vignais 2002; Guichard et al. 2006; Sedeek et al. 2009; DeCoursey 2010). It is likely that the low level of O_2^- produced by NADPH oxidase activity in taste cells maintains the voltage-gated proton channel in the open state accounting for the CT response to HCl. Subsequent modulation of NADPH oxidase activity by targeted genetic and pharmacological manipulations alters, then, CT responses to HCl.

Recently, genes encoding for proton channels have been identified in human, mouse, and in the vase tunicate (*Ciona intestinalis*) (Ramsey et al. 2009; DeCoursey 2010). In the expressed voltage-gated proton channels, the pH-sensitive gating mechanism results in the channel opening when there is an outward electrochemical driving force for protons. So that opening proton channels results in acid extrusion from cells. The above identified voltage-gated proton channels are most likely not involved in CT responses to HCl. In our studies (Lyall et al. 2001), increasing the gradient across the apical membrane of taste cells (i.e., decreasing pH_o by stimulating the tongue with HCl) results in H^+ influx and a subsequent sustained decrease in taste cell pH_i (Lyall et al. 2001). Accordingly, we hypothesize that in taste cells, the proton channels linked to NADPH oxidase must be different from those described in phagocytes and permit the influx of H^+. Alternately, it is possible that the NADPH oxidase–linked proton channels in taste cells may permit H^+ influx when the external pH is decreased below pH 3.0 during stimulation of the apical membrane with HCl. A major difference between taste cells and phagocytes is that in the latter case H^+ for transport is produced intracellularly while during HCl taste stimulation H^+ ions permeate from the apical compartment into taste cells. It is likely that both the intracellular acidification induced by proton flux and the resulting cellular depolarization contribute to the eventual taste receptor cell response to strong acids (Lyall, Alam, Phan, Phan, et al. 2002; Richter et al. 2003; Huang et al. 2008; Chang et al. 2010).

Voltage-gated proton channels demonstrate single channel currents that are about 1000 times smaller than those in most ion channels (Musset et al. 2009). This may explain why stimulating the tongue with HCl, a large decrease in pH_o will produce only a few tenths of a pH unit change in the pH_i of polarized taste cells (Lyall, Alam, Phan, Phan, et al. 2002). That is, the proton conductance of the apical membrane of taste cells is inherently low. In human neutrophils, a decrease in pH_i during phagocytosis inhibits NADPH oxidase activity (Morgan et al. 2009). Inhibition of the NADPH oxidase activity by an acid-induced decrease in the intracellular pH of taste cells beyond a threshold value may be essential in limiting the entry of H^+ through proton channels coupled to NAHPH oxidase activity. The NADPH oxidase–associated proton conductance seems to play a role in eliciting CT responses to strong acids only. Nitrazepam (Figure 4A,B), H_2O_2 (Figure 3C and Supplementary Figure 1B), Zn^{2+} (Figure 1C,D), and DEPC (Supplementary Figure 1B) did not affect CT responses to the weak organic acids (acetic acid and CO_2). These results are consistent with the observations that weak acids, for the most part, enter taste cells across the apical membrane passively as neutral molecules, and once inside the cell, dissociate to generate H^+ intracellularly (Lyall et al. 2001). However, alternate sour taste sensing mechanisms for weak acids have been proposed. A recent study speculated that carbonic anhydrase 4, a glycosylphosphatidylinositol-anchored enzyme, functions as an extracellular H^+ ion generator in the detection of CO_2 in PKD2L1-expressing sour-sensing cells (Chandrashekar et al. 2009).

cAMP PKA–dependent proton conductance in taste cells

Cyclic AMP enhanced the CT response to HCl in rats (Figure 7B,C) and in gp91^{phox} KO mice (Figure 7A). The cAMP-dependent CT response to HCl (Figure 2A; △) demonstrated

a sizable voltage dependence over the entire voltage range from +90 and –90 mV. The relationship between applied voltage across the receptive field and the magnitude of the tonic CT response was quasi-linear. Underlying this is the fact that the cAMP-dependent part of the HCl CT response varied nearly linearly with voltage between ±60 mV while flattening somewhat outside this range on both the positive and negative ends to produce the sigmoid predicted by an ion channel kinetic model (see Appendix and Figure 2A). For the cAMP-dependent part of the response, the respective rate constants for the formation of the channel-H^+ complex and its dissociation are voltage independent suggesting that the cAMP-sensitive proton conductance is also voltage independent. On the other hand, the very nonlinear dependence of the NADPH oxidase–linked part of the HCl CT response on voltage suggests the presence of a voltage-dependent proton conductance. For modeling purposes, just one of several possibilities is a voltage-dependent rate constant for the dissociation of the proton-channel complex as discussed in the Appendix. The CT recordings under voltage clamp, therefore, support a 2-channel hypothesis. One channel (subsequently shown to be linked to NADPH activity) results in a CT response with a nonlinear voltage dependence, whereas a second channel, once activated by cAMP, produces a quasi-linear dependence of response on voltage.

The cAMP-sensitive membrane conductance in taste cells is not gated directly by cAMP but is enhanced by a PKA-dependent mechanism (Figure 7B,C). The cAMP-PKA sensitive channel is distinct from the NADPH oxidase–dependent proton conductance. This conclusion is supported by the observations that in KO mice, the residual NADPH oxidase–independent HCl CT response was enhanced by cAMP and was H_2O_2 insensitive (Figure 7A). Cyclic AMP levels in cells can be regulated by either membrane associated adenylyl cyclases (Abaffy et al. 2003; Clapp et al. 2008) or by phosphodiesterases (Price 1973; McLaughlin et al. 1994; Spickofsky et al. 1994; Moriyama et al. 2002). An increase in intracellular cAMP has been shown to increase influx of Ca^{2+} through L-type voltage-gated Ca^{2+} channels in presynaptic cells (type III cells) (Roberts et al. 2009). An increase in intracellular Ca^{2+} can activate the basolateral Na^+-H^+ exchanger-1 (NHE-1) and, thus, modify the level of adaptation to the sour stimuli (Lyall, Alam, Phan, Phan, et al. 2002; Lyall, Alam, et al. 2004). However, at present, the factors that regulate cAMP levels in taste cells expressing PKD2L1 marker proteins are not known.

In summary, our results show that CT responses to HCl are voltage dependent, are inhibited by proton channel blockers, Zn^{2+} and DEPC, and are enhanced by NADPH oxidase activators H_2O_2, PMA, and nitrazepam. In gp91^{phox} KO mice, the HCl CT response was diminished by about 64% relative to WT mice. The residual response was inhibited by Zn^{2+}, was insensitive to H_2O_2 and, was enhanced by pretreating the tongue with cAMP-dependent PKA activation. We conclude that CT responses to strong acids, such as HCl, are dependent upon 2 proton entry pathways, an NADPH oxidase–dependent proton channel and a cAMP-PKA sensitive proton channel. Consistent with the data presented in this paper and elsewhere (Lyall, Alam, Phan, Phan, et al. 2002; Lyall, Alam, et al. 2004; DeSimone et al. 2007), in a recent study, Chang et al. (2010) identified an apical proton conductance unique to the PKD2L1-expressing acid-sensing taste cells. It is suggested that during sour transduction, protons enter through an apical proton conductance to directly depolarize the taste cell membrane. The results presented in this paper reinforce the idea that the proximate signal for sour taste transduction for strong and weak acids is a decrease in intracellular pH of taste cells (DeSimone and Lyall 2006; Roper 2007). Because rats and WT mice demonstrate strong preference for both blockers of proton channels, Zn^{2+}, and DEPC (Lyall VL, DeSimone JA, unpublished observations and Riera et al. 2009), a direct relation between the apical proton conductances in taste cells and behavioral responses to strong acids could not be determined. Although our PCR data clearly demonstrate that gp91^{phox} can be found in FF taste cells (Supplemental Figure 4), further studies are needed to demonstrate that NADPH oxidase–dependent and –independent proton conductances are localized specifically in sour-sensing taste cells that express the PKD2L1 marker protein and if the factors that modulate proton conductances have any effect in neural responses in PKD2L1 KO mice.

Supplementary material

Supplementary material can be found at http://www.chemse.oxfordjournals.org/.

Funding

This work was supported by the National Institute on Deafness and other Communication Disorders grants (DC-000122 and DC-005981) to VL.

Appendix

Ion channel kinetic model

The significantly altered voltage dependence of the rat CT response to HCl following the application of cAMP to the tongue in addition to an increase in response magnitude is consistent with a role for 2 distinct taste cell H^+ channels participating in the detection of H^+ ions. One H^+ channel is activated by NADPH oxidase, whereas the other channel is independent of NADPH oxidase but shows increased conductance in the presence of cAMP. To fit the CT response data as a function of clamped lingual voltage, we have made use of a standard ion channel kinetic model (Mintz et al. 1986). Accordingly, J_H, the flow of H^+ across the taste cell apical membrane, is modeled as

$$J_H = \frac{k_0 N c_H e^{-\theta/2}}{c_H e^{-\theta/2} + K_m(1+e^{\theta/2})} \quad (1)$$

Here, k_0 is the dissociation rate constant of the channel-H^+ complex, N is the total number of channels, c_H is the stimulus H^+ ion concentration (which at 20 mM is much higher than the intracellular H^+ concentration), θ is the normalized potential difference across the taste cell apical membrane (FV_a/RT, where V_a is the potential across the apical membrane and F, R, and T have their usual thermodynamic meaning), and $K_m = k_0/f_0$, where f_0 is the association rate constant for the formation of the channel-H^+ complex.

We assume the CT response, R, is proportional to J_H and that $\theta = \delta\varphi$, where φ is the normalized translingual epithelial potential difference and δ is the fraction of φ dropped across the apical membrane. The curve in Figure 2C showing the fit to the cAMP-sensitive part of the CT response as a function of applied transepithelial potential was, accordingly, obtained from

$$R = \frac{R_m a e^{-\delta\varphi/2}}{a e^{-\delta\varphi/2} + (1+e^{\delta\varphi/2})} \quad (2)$$

where R_m is the maximum CT response and $a = c_H/K_m$.

To fit the data in Figure 2C showing the voltage dependence of the CT response in the absence of added cAMP, required the additional assumption that beyond a threshold potential, τ, k_0 can increase, that is, H^+ ions can dissociate more easily from the channel as the potential becomes increasingly negative. This was modeled using

$$k_0 = k_{00}\left(1 + e^{-n(\varphi-\tau)}\right) \quad (3)$$

where k_{00} and n are positive constants. Accordingly, the data in Figure 2C were fitted to

$$R = \frac{\beta a e^{-\delta\varphi/2}\left(1+e^{-n(\varphi-\tau)}\right)}{a e^{-\delta\varphi/2} + \left(1+e^{-n(\varphi-\tau)}\right)\left(1+e^{\delta\varphi/2}\right)} \quad (4)$$

where β is a positive constant.

The H^+ channel blockers, Zn^{2+} and DEPC, were reversible inhibitors of the CT response to HCl but did not inhibit responses to acetic acid and CO_2. Their effects on the CT response to HCl were modeled assuming that each is a competitive inhibitor of the H^+ ion flux through the H^+ channels. The model was generalized to include the possibility of more than one Zn^{2+}- or DEPC-binding site per channel. The resulting fit equation for Zn^{2+} was

$$R = \frac{R_m}{1 + c_{Zn}^n / k^n} \quad (5)$$

where R is the CT response to 20 mM HCl containing concentration, c_{Zn} of Zn^{2+}, R_m is the maximum response, k is the Zn^{2+} concentration at which R is inhibited by 50%, and n is a positive constant equal to or greater than one. The data obtained with DEPC were fit to a similar equation (cf. Figure 1B).

H_2O_2 enhanced the response of HCl in a concentration-dependent manner. Specifically, the response was a saturating sigmoidal function of H_2O_2 concentration (Hill equation). Accordingly, the data points in Figure 3B were fitted to

$$R = \frac{R_1 c^n}{k_{0.5}^n + c^n} + R_0 \quad (6)$$

where R is the CT response to 20 mM HCl containing concentration, c of H_2O_2, R_0 is the response to HCl in the absence of H_2O_2, R_1 is the maximum additional response due to H_2O_2, $k_{0.5}$ is the H_2O_2 concentration at which R relative to R_0 reaches 50% of R_1, and n is a positive constant equal to or greater than one.

References

Abaffy T, Trubey KR, Chaudhari N. 2003. Adenylate cyclase expression and modulation of cAMP in rat taste cells. Am J Physiol Cell Physiol. 284:C1420–C1429.

Abramov AY, Jacobson J, Wientjes F, Hothersall J, Canevari L, Duchen MR. 2005. Expression and modulation of an NADPH oxidase in mammalian astrocytes. J Neurosci. 25:9176–9184.

Botelho LHP, Rothermel JD, Coombs RV, Jastorff B. 1988. Cyclic AMP analog antagonists of cAMP action. Methods Enzymol. 159:159–172.

Chandrashekar J, Yarmolinsky D, von Buchholtz L, Oka Y, Sly W, Ryba NJ, Zuker CS. 2009. The taste of carbonation. Science. 326(5951):443–445.

Chang RB, Waters H, Liman ER. 2010. A proton current drives action potentials in genetically identified sour taste cells. Proc Natl Acad Sci U S A. 107:22320–22325.

Clapp TR, Trubey KR, Vandenbeuch A, Stone LM, Margolskee RF, Chaudhari N, Kinnamon SC. 2008. Tonic activity of Gα-gustducin regulates taste cell responsivity. FEBS Lett. 582:3783–3787.

Clement H-W, Vazquez JF, Sommer O, Heiser P, Morawietz H, Hopt U, Schulz E, Dobschutz EV. 2010. Lipopolysaccharide-induced radical formation in the striatum is abolished in Nox2 $gp91^{phox}$-deficient mice. J Neural Transm. 117:13–22.

DeCoursey TE. 2003. Voltage-gated proton channels and other proton transfer pathways. Physiol Rev. 25:27–40.

DeCoursey TE. 2010. Voltage-gated proton channels find their dream job managing the respiratory burst in phagocytes. Physiology. 25:27–40.

DeSimone JA, Callaham EM, Heck GL. 1995. Chorda tympani taste response of rat to hydrochloric acid subject to voltage-clamped lingual receptive field. Am J Physiol Cell Physiol. 268:C1295–C1300.

DeSimone JA, Lyall V. 2006. Taste receptors in the gastrointestinal tract III. Salty and sour taste: sensing of sodium and protons by the tongue. Am J Physiol Gastrointest Liver Physiol. 291:G1005–G1010.

DeSimone JA, Phan THT, Heck GL, Mummalaneni S, Sturz GR, Lyall V. 2007. Proton flux through NADPH oxidase-linked H^+ channel ($gp91^{phox}$) is involved in eliciting chorda tympani (CT) taste nerve responses to strong acids [abstract]. Chem Senses. 32:A22.

Guichard C, Pedruzzi E, Fay M, Ben Mkaddem S, Coant N, Daniel F, Ogier-Denis E. 2006. The Nox/Duox family of ROS-generating NADPH oxidases. Med Sci (Paris). 22:953–960.

Horio N, Yoshida R, Ishimaru Y, Matsunami H, Ninomiya Y. 2010. PKD2L1 is required for normal chorda tympani nerve responses to acids [abstract]. Chem Senses. 35:A63.

Huang AL, Chen X, Hoon MA, Chandrashekar J, Guo W, Tränkner D, Ryba NJP, Zuker CS. 2006. The cells and logic for mammalian sour taste detection. Nature. 442:934–938.

Huang YA, Maruyama Y, Stimac R, Roper SD. 2008. Presynaptic (Type III) cells in mouse taste buds sense sour (acid) taste. J Physiol. 586: 2903–2912.

Huque T, Cowart BJ, Dankulich-Nagrudny L, Pribitkin EA, Bayley DL, Spielman AI, Feldman RS, Mackler SA, Brand JG. 2009. Sour ageusia in two individuals implicates ion channels of the ASIC and PKD families in human sour taste perception at the anterior tongue. PLoS One. 4(10):e7347.

Ishimaru Y, Inada H, Kubota M, Zhuang H, Tominaga M, Matsunami H. 2006. Transient receptor potential family members PKD1L3 and PKD2L1 form a candidate sour taste receptor. Proc Natl Acad Sci U S A. 103:12569–12574.

Ishimaru Y, Matsunami H. 2009. Transient receptor potential (TRP) channels and taste sensation. J Dent Res. 88:212–218.

Kataoka S, Yang R, Ishimaru Y, Matsunami H, Sévigny J, Kinnamon JC, Finger TE. 2008. The candidate sour taste receptor, PKD2L1, is expressed by type III taste cells in the mouse. Chem Senses. 33:243–254.

Liu JQ, Zelko IN, Erbynn EM, Sham JSK, Folz RJ. 2006. Hypoxic pulmonary hypertension: role of superoxide and NADPH oxidase ($gp91^{phox}$). Am J Physiol Lung Cell Mol Physiol. 290:L2–L10.

LopezJimenez ND, Cavenagh MM, Sainz E, Cruz-Ithier MA, Battey JF, Sullivan SL. 2006. Two members of the TRPP family of ion channels, Pkd1l3 and Pkd2l1, are co-expressed in a subset of taste receptor cells. J Neurochem. 98:68–77.

Lyall V, Alam RI, Malik SA, Phan THT, Vinnikova AK, Heck GL, DeSimone JA. 2004. Basolateral Na^+-H^+ exchanger-1 in rat taste receptor cells is involved in neural adaptation to acidic stimuli. J Physiol. 556:159–173.

Lyall V, Alam RI, Phan DQ, Ereso GL, Phan THT, Malik SA, Montrose MH, Chu S, Heck GL, Feldman GM, et al. 2001. Decrease in rat taste receptor cell pH is the proximate stimulus in sour taste transduction. Am J Physiol Cell Physiol. 281:C1005–C1013.

Lyall V, Alam RI, Phan THT, Phan DQ, Heck GL, DeSimone JA. 2002. Excitation and adaptation in the detection of hydrogen ions by taste receptor cells: a role for cAMP and Ca^{2+}. J Neurophysiol. 87:399–408.

Lyall V, Alam RI, Phan THT, Russell OF, Malik SA, Heck GL, DeSimone JA. 2002. Modulation of rat chorda tympani NaCl responses and intracellular Na^+ activity in polarized taste receptor cells by pH. J Gen Physiol. 120:793–815.

Lyall V, Heck GL, Vinnikova AK, Ghosh S, Phan THT, Alam RI, Russell OF, Malik SA, Bigbee JW, DeSimone JA. 2004. The mammalian amiloride-insensitive non-specific salt taste receptor is a vanilloid receptor-1 variant. J Physiol. 558:147–159.

Lyall V, Pasley H, Phan THT, Mummalaneni S, Heck GL, Vinnikova AK, DeSimone JA. 2006. Intracellular pH modulates taste receptor cell volume and the phasic part of the chorda tympani response to acids. J Gen Physiol. 127:15–34.

Lyall V, Phan THT, Mummalaneni S, Melone P, Mahavadi S, Murthy KS, DeSimone JA. 2009. Regulation of the benzamil-insensitive salt taste receptor by intracellular Ca^{2+}, protein kinase C and calcineurin. J Neurophysiol. 102:1591–1605.

Malech HL. 1999. Progress in gene therapy for chronic granulomatous disease. J Infect Dis. 179:S318–S325.

Mankelow TJ, Henderson LM. 2001. Inhibition of the neutrophil NADPH oxidase and associated H^+ channel by diethyl pyrocarbonate (DEPC), a histidine-modifying agent: evidence for at least two target sites. Biochem J. 358:315–324.

McLaughlin SK, McKinnon PJ, Spickofsky N, Danho W, Margolskee RF. 1994. Molecular cloning of G proteins and phosphodiesterases from rat taste cells. Physiol Behav. 56:1157–1164.

Mintz E, Thomas SR, Mikulecky DC. 1986. Exploration of the apical sodium transport mechanisms in an epithelial model by network thermodynamic simulation of the effect of mucosal sodium depletion: II An apical sodium channel and amiloride blocking. J Theor Biol. 123:21–34.

Morgan D, Capasso M, Musset B, Cherny VV, Rios E, Dyer MJS, DeCoursey TE. 2009. Voltage-gated proton channels maintain pH in human neutrophis during phagocytosis. Proc Natl Acad Sci U S A. 106:18022–18027.

Moriyama K, Bakre MM, Ahmed F, Spickofsky N, Max M, Margolskee RF. 2002. Assaying G protein-phosphodiesterase interactions in sensory systems. Methods Enzymol. 345:37–48.

Musset B, Cherny VV, Morgan D, DeCoursey TE. 2009. The intimate and mysterious relationship between proton channels and NADPH oxidase. FEBS Lett. 583:7–12.

Musset B, Smith SME, Rajan S, Cherny VV, Sujai S, Morgan D, DeCoursey TE. 2010. Zinc inhibition of monomeric and dimeric proton channels suggests cooperative gating. J Physiol. 588:1435–1449.

Nelson TM, LopezJimenez ND, Tessarollo L, Inoue M, Bachmanov AA, Sullivan SL. 2010. Taste function in mice with a targeted mutation of the pkd1l3 gene. Chem Senses. 35:565–577.

Price S. 1973. Phosphodiesterases in tongue epithelium: activation by bitter taste stimuli. Nature. 241:54–55.

Ramsey IS, Ruchti E, Kaczmarek JS, Clapham DE. 2009. Hv1 proton channels are required for high-level NADPH oxidase-dependent superoxide production during the phagocyte respiratory burst. Proc Natl Acad Sci U S A. 106:7642–7647.

Richter TA, Caicedo A, Roper SD. 2003. Sour taste stimuli evoke Ca^{2+} and pH responses in mouse taste cells. J Physiol. 547:475–483.

Riera CE, Vogel H, Simon SA, Damak S, le Coutre J. 2009. Sensory attributes of complex tasting divalent salts are mediated by TRPM5 and TRPV1 channels. J Neurosci. 29:2654–2662.

Roberts CD, Dvoryanchikov G, Roper SD, Chaudhari N. 2009. Interaction between the second messengers cAMP and Ca^{2+} in mouse presynaptic taste cells. J Physiol. 587:1657–1668.

Roper SD. 2007. Signal transduction and information processing in mammalian taste buds. Pflűgers Arch. 454:759–776.

Rosen GM, Rauckman EJ, Wilson RL Jr, Tschanz C. 1984. Production of superoxide during the metabolism of nitrazepam. Xenoriotica. 14: 785–794.

Sedeek M, Hebert RL, Kennedy CR, Burns KD, Touyz RM. 2009. Molecular mechanisms of hypertension: role of Nox family NADPH oxidases. Curr Opin Nephrol Hypertens. 18:122–127.

Seebungkert B, Lynch JW. 2001. A common inhibitory binding site for zinc and odorants at the voltage-gated K^+ channel of rat olfactory receptor neurons. Eur J Neurosci. 14:353–362.

Spickofsky N, Robichon A, Danho W, Fry D, Greeley D, Graves B, Madison V, Margolskee RF. 1994. Biochemical analysis of the transducin-phosphodiesterase interaction. Nat Struct Biol. 1:771–781.

Stewart RE, Lyall V, Feldman GM, Heck GL, DeSimone JA. 1998. Acid-induced responses in hamster chorda tympani and intracellular pH (pHi) tracking by taste receptor cells. Am J Physiol Cell Physiol. 275: C227–C238.

Vignais PV. 2002. The superoxide-generating NADPH oxidase: structural aspects and activation mechanism. Cell Mol Life Sci. 59:1428–1459.

Wu DC, Ré DB, Nagai M, Ischiropoulos H, Przedborski S. 2006. The inflammatory NADPH oxidase enzyme modulates motor neuron degeneration in amyotrophic lateral sclerosis mice. Proc Natl Acad Sci U S A. 103:12132–12137.

Ye Q, Heck GL, DeSimone JA. 1991. The anion paradox in sodium taste reception: resolution by voltage-clamp studies. Science. 254(5032):724–726.

Yoshida R, Miyauchi A, Yasuo T, Jyotaki M, Murata Y, Yasumatsu K, Shigemura N, Yanagawa Y, Obata K, Ueno H. 2009. Discrimination of taste qualities among mouse fungiform taste bud cells. J Physiol. 587:4425–4439.